TISSUE ENGINEERING: Part A
Volume 21, Numbers 11 and 12, 2015

DOI: 10.1089/ten.tea.2014.0511

Fate of Distal Lung Epithelium Cultured in a Decellularized Lung Extracellular Matrix

Elizabeth A. Calle, MPhil,[1] Julio J. Mendez, PhD,[2] Mahboobe Ghaedi, PhD,[2] Katherine L. Leiby, BS,[1] Peter F. Bove, PhD,[3] Erica L. Herzog, MD, PhD,[4] Sumati Sundaram, PhD,[2] and Laura E. Niklason, MD, PhD[1,2]

Type II cells are the defenders of the alveolus. They produce surfactant to prevent alveolar collapse, they actively transport water to prevent filling of the air sacs that would otherwise prevent gas exchange, and they differentiate to type I epithelial cells. They are an indispensable component of functional lung tissue. To understand the functionality of type II cells in isolation, we sought to track their fate in decellularized matrices and to assess their ability to contribute to barrier function by differentiation to type I alveolar epithelial cells. Rat type II cells were isolated from neonatal rat lungs by labeling with the RTII-70 surface marker and separation using a magnetic column. This produced a population of ~50% RTII-70-positive cells accompanied by few type I epithelial cells or α-actin-positive mesenchymal cells. This population was seeded into decellularized rat lung matrices and cultured for 1 or 7 days. Culture in Dulbecco's modified Eagle's medium +10% fetal bovine serum (FBS) resulted in reduced expression of epithelial markers and increased expression of mesenchymal markers. By 7 days, no epithelial markers were visible by immunostaining; nearly all cells were α-actin positive. Gene expression for the mesenchymal markers, *α-actin*, *vimentin*, and *TGF-βR*, was significantly upregulated on day 1 ($p = 0.0005$, 0.0005, and 2.342E-5, respectively). Transcript levels of *α-actin* and *TGF-βR* remained high at 7 days ($p = 1.364E-10$ and 0.0002). Interestingly, human type II cells cultured under the same conditions showed a similar trend in the loss of epithelial markers, but did not display high expression of mesenchymal markers. Rat cells additionally showed the ability to produce and degrade the basement membrane and extracellular matrix components, such as fibronectin, collagen IV, and collagen I. Quantitative real-time reverse transcription polymerase chain reaction (RT-PCR) showed significant increases in expression of the *fibronectin* and *matrix metalloprotease-2* (MMP-2) genes after 1 day in culture ($p = 0.0135$ and 0.0128, respectively) and elevated *collagen I* expression at 7 days ($p = 0.0016$). These data suggest that the original type II-enriched population underwent a transition to increased expression of mesenchymal markers, perhaps as part of a survival or wound-healing program. These results suggest that additional medium components and/or the application of physiologically appropriate stimuli such as ventilation may be required to promote lung-specific epithelial phenotypes.

Introduction

In recent years, several laboratories have reported the repopulation of decellularized lung matrices with mixed populations of differentiated cells or with precursor-derived or stem cell-derived cells.[1–7] Previous data indicate the ability of a mixed population of rat neonatal lung cells to repopulate an acellular lung extracellular matrix (ECM) scaffold in a regionally specific manner. When a decellularized lung ECM scaffold was seeded with a mixed population of neonatal lung cells, pro-surfactant protein-C (pro-SPC)-positive type II epithelial cells tended to locate in the vertices of the alveoli with morphologically appropriate expression of pro-SPC; they were generally not found in more proximal airway structures.[2]

When provided with breathing movements inside of a bioreactor, the mixed neonatal cells also were able to populate the alveoli with type I pneumocytes and the proximal airways with appropriate proximal lung epithelial cell types, including club cells and rare basal cells. To understand the localization and differentiation capacity of a single cell type from the previous mixed populations, we enriched for type

[1]Department of Biomedical Engineering, Yale University, New Haven, Connecticut.
[2]Department of Anesthesia, Yale University School of Medicine, New Haven, Connecticut.
[3]Cystic Fibrosis/Pulmonary Research Treatment Center, University of North Carolina, Chapel Hill, North Carolina.
[4]Section of Pulmonary, Critical Care, and Sleep Medicine, Department of Internal Medicine, Yale University School of Medicine, New Haven, Connecticut.

II alveolar epithelial cells from a mixed rat epithelial population. We evaluated the capacity of the type II population to adhere to, proliferate within, and reconstitute the alveoli *in vitro*. Type II cells serve the critical functions of surfactant production, alveolar fluid transport, and differentiation to type I cells. Indeed, work by Lwebuga-Mukasa *et al.*, wherein isolated rat type II cells were cultured on slices of decellularized human lung matrix *in vitro*, suggested that type II cells would undergo a transition to a type I alveolar epithelial-like phenotype, as assessed by morphological changes observed with electron microscopy.[8]

In this study, we describe the isolation of a distal lung epithelial cell population that is enriched for RTII-70-positive cells and the subsequent seeding and cultivation of these cells in decellularized lung scaffolds. RTII-70 is a surface marker of type II epithelial cells in the adult rat lung[9] and has been used successfully to isolate nearly pure populations of RTII-70+ cells through fluorescence-activated cell sorting (FACS).[10,11] The cell populations isolated here, from neonatal rat pups that were 7–10 days old, were ~50% positive for RTII-70 and most of these cells were also positive for the type II pneumocyte marker, pro-SPC.

Our data show that this RTII-70+ population was able to adhere to the matrix after seeding onto the scaffolds and spending 1 day in culture. These cells persist within the scaffold for at least 7 days. Immunostaining and polymerase chain reaction (PCR) data indicate a significant decline in the RTII-70 marker that was used to enrich the isolate as well as other alveolar epithelial markers, such as pro-SPC and AQP-5, with increased time in culture. There was a concomitant increase in mesenchymal markers such as α-actin and vimentin over the course of 7 days. Expression of genes for *collagen I*, *fibronectin*, *matrix metalloprotease-2* (MMP-2), and TGF-β receptor I also increased between seeding time and after 1 week in culture. Taken together, these data suggest that the cells take on a migratory, contractile, and matrix-secreting phenotype atypical of epithelial cells.

The data collected in these studies suggest that the alveolar epithelial cells that are isolated and cultured in a bioreactor in the presence of FBS undergo an epithelial-to-mesenchymal transition, likely as a part of the wound healing required to repopulate an acellular matrix in the presence of serum. This is a somewhat surprising finding since mixed populations of neonatal rat cells, on the same scaffold and in the same serum-containing media, do not demonstrate this type of transition. This suggests that mixtures of cell types, especially if they include niche-supporting mesenchymal cells, may in fact result in retention of epithelial phenotype better than type II cells cultured in relative isolation.

Materials and Methods

All animal work was done in accordance with AAALAC and AVMA guidelines and was approved by the Yale IACUC.

Lung decellularization and scaffold preparation

Lungs were obtained from anesthetized 3–4-month-old adult Fischer 344 rats as previously described.[12] Briefly, lungs were cleared of blood *in situ*, and the lungs, heart, and trachea were removed *en bloc*. The pulmonary artery and trachea were cannulated, and lungs were mounted in a bioreactor for decellularization. After treatment with 500 mL of decellularization solution containing 8 mM CHAPS, lungs were inflated with benzonase endonuclease (90 U/mL), incubated for 1 h at 37°C, and rinsed extensively with phosphate-buffered saline (PBS). Lungs were then perfused with antibiotics/antimycotics for up to 72 h at room temperature and stored at 4°C until use.

In preparation for seeding, lungs were removed from the bioreactor in a sterile manner. The left lung and three of the four lobes of the right lung were removed, leaving only the upper right lobe connected to the trachea and pulmonary artery. The lobe was then replaced into the bioreactor for seeding with isolated lung cells.

Rat distal lung epithelial cell isolation

Cells were isolated according to a protocol adapted from Rice *et al.*[13] Seven-day-old Sprague-Dawley rat pups were euthanized by IP injection of sodium pentobarbital (150 mg/kg). Then, the chest plate was removed, the apex of the heart severed, and the lungs cleared of blood with 100 U/mL heparin in PBS. The trachea was dissected out and cannulated with a 24 G, 0.75-in I.V. catheter. The lungs were inflated with 1.0–1.5 mL dispase (2 U/mL) in Dulbecco's modified Eagle's medium (DMEM) with 20% HBSS, followed by ~0.5 mL of 1% low-melting-point agarose. The lungs were covered with ice to allow the agarose to gel, and then the lungs were removed from the chest and incubated with additional dispase solution (1 mL/set of lungs) for 45 min at room temperature.

After incubation, lungs were transferred to a Petri dish containing DMEM with 1% HEPES and 100 U/mL DNAse I. In this study, the lung tissue was teased apart and the mainstem bronchi removed. The remaining tissue was minced, then dissociated with a blunt bone marrow aspiration needle. The homogenized tissue was then filtered with 100- and 40-μm cell strainers and through a 20-μm mesh and treated with antibiotics/antimycotics. The cell suspension was centrifuged and partitioned for cell labeling and positive selection.

Positive cell selection with RTII-70 monoclonal antibody

Suspended cells were labeled with RTII-70 antibody at 1:40 dilution.[9] After incubating with primary antibody for 30 min at room temperature in DMEM with 2 mM EDTA and 0.5% BSA (hereafter, labeling buffer), labeled cells were washed and incubated with anti-mouse IgG superparamagnetic microbeads from Miltenyi Biotec for 25 min at 4°C. Labeled and tagged cells were washed and resuspended in 500 μL of labeling buffer per 60 million cells. MS columns were positioned in a magnetic field and rinsed with 500 μL of labeling buffer. Five hundred microliters of cell suspension was then applied to each column. Columns were subsequently rinsed with additional labeling buffer, then removed from the magnet, and flushed to obtain the positively selected RTII-70-positive labeled cells.

Bioreactor seeding and culture of RTII-70+ cells in mounted decellularized matrices

Immediately after isolation and positive selection, 10 million cells were introduced to the upper right lobe of the decellularized lung that was mounted in the bioreactor. Cells were injected into the lobe using a 3-mL syringe containing

1.5 mL of cells suspended in DMEM + 10% fetal bovine serum (FBS) + 1% penicillin/streptomycin (hereafter referred to as culture medium). The injection was followed by a slow infusion of media into the lobe through the airways. The infusion was the result of generating negative pressure in the main bioreactor chamber with a syringe pump. The pump removed a total of 30 mL of air from the main bioreactor jar, which allowed the lung to fill with media from the trachea reservoir. The syringe pump removed air at 2 mL/min.

Lungs remained static (no perfusion, no ventilation) overnight at 37°C and 5% CO_2. Pulsatile perfusion of 1 mL/min was initiated 16–24 h after seeding and continued for the remainder of the culture period.

Bioreactor seeding and culture of human type II cells in mounted decellularized matrices

Human type II epithelial cells were obtained from Dr. Peter Bove at the University of North Carolina (Chapel Hill, NC) and have been previously characterized.[14] Decellularized lungs were prepared as described and the upper right lobe, connected to the trachea, was mounted in the bioreactor for seeding and culture. A total of 6–7 million human type II cells were seeded into each bioreactor-mounted lobe and cultured as described for the rat cells. Samples were harvested at 7 days. Each sample was divided in half for RNA analysis and histology and immunohistochemistry (IHC).

Fluorescence-activated cell sorting

Single cell suspensions were fixed in 2% paraformaldehyde (PFA) for 10 min at room temperature. They were stored in 0.6% PFA at 4°C for up to 2 weeks. The fixed cells were washed with PBS, followed by incubation with primary antibodies in blocking solution (10% FBS, 0.2% Triton X-100, in PBS) for 25 min on ice. Primary antibodies against SPC (1:500, AB3786; Millipore), AQP5 (1:100, AB3559; Millipore), and α-SMA (1:100; Abcam) were used. Appropriate isotypes and/or secondary controls used included anti-mouse IgG APC (12-4714; ebiosciences) and purified anti-rabbit IgG (02-6102; Invitrogen).

The cells were then washed twice with PBS and incubated with species-specific secondary antibodies for an additional 25 min on ice. Finally, the cells were washed as above and resuspended in PBS for analysis with the BD-FACS Aria.

Quantitative real-time reverse transcription polymerase chain reaction

Quantitative real-time reverse transcription polymerase chain reaction (qRT-PCR) was performed to determine the expression of epithelial and mesenchymal markers. Briefly, total cellular RNA was prepared using the RNeasy Mini Kit following the manufacturer's instructions (Qiagen). Single-stranded cDNA was synthesized using the SuperScript First-Strand Synthesis System according to the manufacturer's protocol (Invitrogen). An equal volume mixture of the cDNA was used as a template for PCR amplification. All PCR reactions were done in triplicate in a 25 mL volume with iQ SYBR Green Supermix (Bio-Rad) and 200 nM each of forward and reverse primers listed in Table 1. Concentrations of all primers were optimized before use. Real-time quantitative PCR was performed on iCyler and iQ software (Bio-Rad), with an initial denaturation step of 4 min at 95°C, followed by 40 cycles of PCR consisting of 15 s at 95°C, 30 s at 60°C, and 30 s at 72°C. Average threshold cycle (Ct) values from the triplicate PCR reactions for a gene of interest (GOI) were normalized against the average Ct values for GAPDH from the same cDNA sample. Fold change of GOI transcript levels between sample A and sample B equals $2^{-\Delta\Delta Ct}$, where $\Delta Ct = Ct_{(GOI)} - Ct_{(GAPDH)}$ and $\Delta\Delta Ct = \Delta Ct_{(A)} - \Delta Ct_{(B)}$.

Table 1. Primers Used for Real-Time Quantitative Reverse Transcription–Polymerase Chain Reaction on Rat Cells and Tissue

Gene	*Length (bp)*	*Primer sequences*
SPC	114	Forward: CTCCTGACCGCCTATAAGC Reverse: TGGCCTGGAAGTTCTTGAAT
AQ5	182	Forward: CCTCTCACTGGGTCTTCTGG Reverse: GCTCGATGGTCTTCTTCCTCT
α-ACTIN	133	Forward: GCTTTGCTGGTGATGATGCT Reverse: GATCCCTCTCTTGCTCTGC
VIMEN	113	Forward: TGAGATCCAGAACATGAAGG Reverse: TCCAGCAGCTTCCTGTAGGT
TGFBR	95	Forward: CTAATGGTGGACCGCAACAAC Reverse: TGCTTCCCGAATGTCTGAC
COLIA1	97	Forward: GAGCGGAGAGTACTGGATCG Reverse: TGGGGAACACACAGGTCTGA
MMP2	114	Forward: AGGGAATGAGTACTGGGTCTAT Reverse: CTCCAGTTAAAGGCAGCGTCT
FIB	208	Forward: TTATGACGACGGGAAGACCT Reverse: TAGTGTTCGTTCTCTGATGGTA
β-actin	128	Forward: GCAGGAGTACGATGAGTCCG Reverse: ACGCAGCTCAGTAACAGTCC

Statistical analyses

PCR data are shown as mean ± SEM. Comparisons were made with Student's *t*-tests, and a *p*-value of < 0.05 was considered statistically significant. Asterisks denote comparison with control. A single asterisk (*) indicates $p < 0.05$, double asterisk (**) indicates $p < 0.01$.

Histology and IHC

After culture, the lobe was removed from the bioreactor and divided approximately in half. The distal portion was frozen for RNA analysis and the proximal portion was inflation fixed with 10% neutral buffered formalin for 2–4 h and transferred to 70% ethanol. The tissue was processed and paraffin embedded. Five-micrometer sections were cut and stained for hematoxylin and eosin (H&E) or saved for IHC.

Tissue sections were baked for 30 min at 65°C, deparaffinized in xylenes, and rehydrated in an ethanol gradient. Sections were subjected to heat-mediated citric acid antigen retrieval at 75°C for 25 min and cooled to room temperature. After rinsing with PBS, sections were permeabilized with 0.2% Triton-X 100 in PBS for 10–12 min at room temperature. Permeabilized sections were blocked with PBS containing 5% BSA and 0.75% glycine for 1 h at room temperature and incubated with primary antibodies overnight at 4°C. Antibody for RTII-70 was applied at 1:40; pro-SPC, 1:1000; aquaporin-5, 1:1000; collagen IV, 1:500; fibronectin, 1:100; MMP-2, 1:500; α-actin, 1:1000; and vimentin, 1:200.

Sections were rinsed and secondaries applied at 1:500 for 1 h at room temperature. Sections were stained with 4′,6-diamidino-2-phenylindole (DAPI) and mounted with polyvinyl alcohol with DABCO (PVA-DABCO), coverslipped, and dried overnight. Stained sections were imaged with a Zeiss Axiovert zoom inverted microscope, a Hamamatsu camera, and Volocity software.

Results

Characterization of isolated neonatal lung cells

Isolation of RTII-70+ cells using positive selection through the Miltenyi system yielded a mean of 40±20 million (SD) RTII-70+ cells per 7-day-old pup (Fig. 1A). For a whole litter, the average number of total RTII-70+ cells was 40 million, a yield of ~8% of the total cells isolated per litter; the initial total comprised ~50% macrophages (data not shown).

The freshly isolated cells were evaluated for expression of type II and type I epithelial cell markers at both the protein and gene levels. We also assayed for markers of mesenchymal cells. For type II cells, we probed for RTII-70[9] and pro-SPC, an intracellular marker for type II pneumocytes or their precursors. For type I epithelial cells, we evaluated expression of AQP-5. By FACS (example of a typical isolation shown in Fig. 1C), 40–52% of the magnetically sorted population is positive for the RTII-70. The

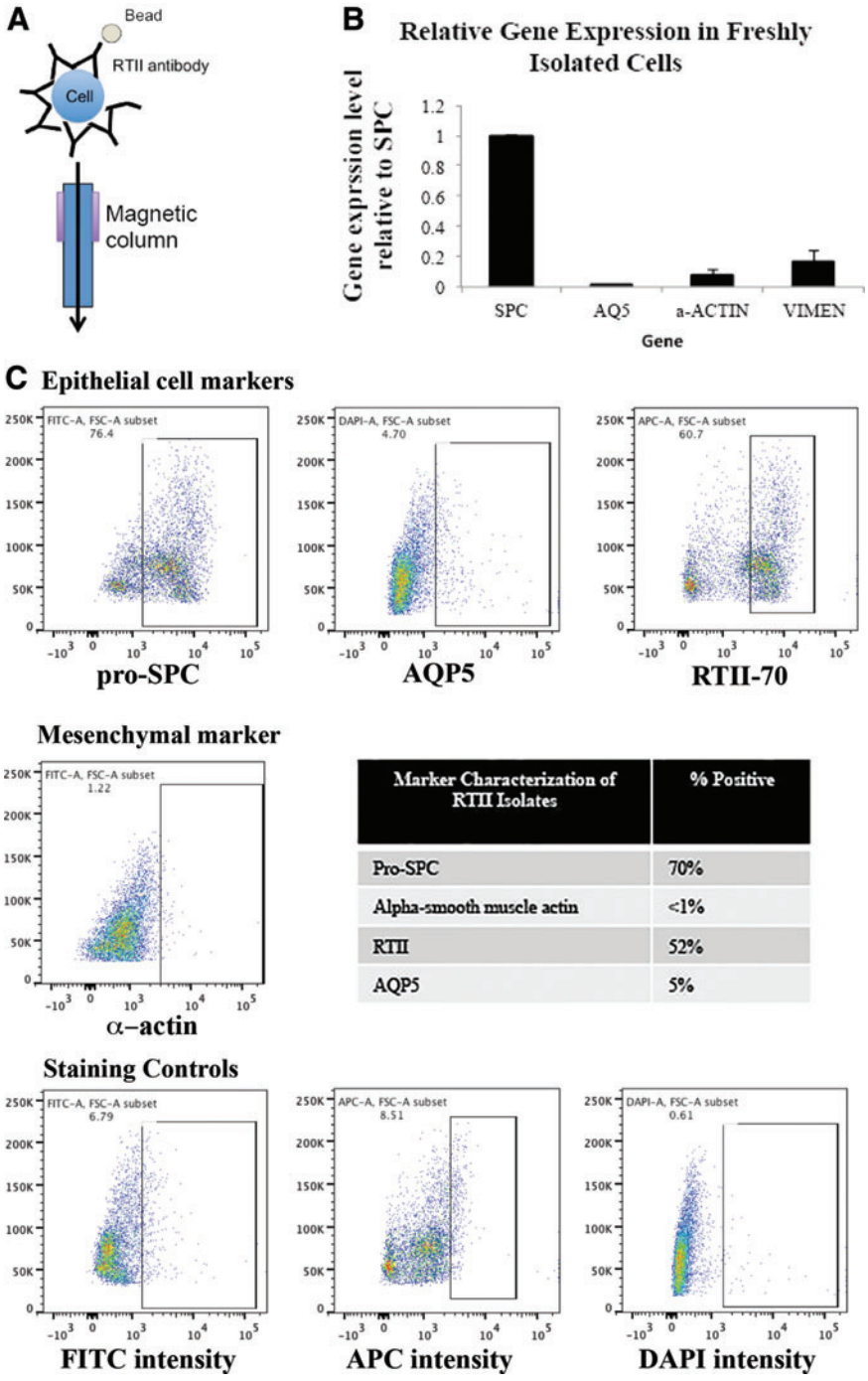

Marker Characterization of RTII Isolates	% Positive
Pro-SPC	70%
Alpha-smooth muscle actin	<1%
RTII	52%
AQP5	5%

FIG. 1. Isolation of RTII-70+ neonatal epithelial cells. **(A)** Cells within a mixed lung cell population are tagged with a primary antibody against RTII-70, followed by a secondary that is conjugated to an iron oxide particle. This allows for separation of the tagged (RTII-70-positive) cells to be separated from the overall population. **(B)** Relative gene expression for alveolar epithelial (*SPC* and *AQP-5*) and mesenchymal (*α-actin* and *vimentin*) markers. **(C)** Fluorescence-activated cell sorting (FACS) analysis of cells separated by magnetic column. Cells are >50% RTII-70 positive. The majority is positive for pro-surfactant protein C (pro-SPC; 70%). Fewer than 1% of cells are positive for α-actin. Very few are aquaporin 5 (AQP-5) positive (4%). Color images available online at www.liebertpub.com/tea

majority of the isolated cells (55–70%) are also pro-SPC+. This portion of pro-SPC+ cells is substantially greater than that found in mixed neonatal isolates, which are obtained by treatment with collagenase and elastase, without sorting (data not shown). Very few of the RTII-70 antibody and bead-isolated cells (4.0% of total) were AQP5 positive, and the abundance of *AQP5* is significantly less than that of *SPC* at the RNA level ($p = 0.0052$; Fig. 1B).

Only <1% of cells were positive for alpha smooth muscle actin by FACS (Fig. 1C). Comparatively, normal mixed cell isolation obtained after elastase/collagenous digestion without sorting includes up to 30% α-actin-positive cells by FACS analysis (data not shown). To further evaluate mesenchymal cell phenotypes, we performed RT-PCR for *alpha actin* and *vimentin*.[15] Gene expression of both *α-actin* and *vimentin* in the bead-sorted cell population is significantly lower than expression of *SPC*, but not completely absent (Fig. 1B). Expression of *α-actin* is 13-fold less than that of SPC, ($p = 0.0072$) and expression of *vimentin* is 6-fold less ($p = 0.01$).

Taken together, these data indicate that magnetic bead isolation for RTII-70 allows for the enrichment of distal lung epithelial cells when compared with whole lung isolates. Use of the RTII-70 surface marker and magnetic bead separation also allows for enrichment of distal epithelium and depletes cells that express mesenchymal cells.

Culture of isolated neonatal RTII-70+ cells on decellularized matrices that are mounted in a bioreactor

To evaluate the initial distribution of cells within the scaffold and their ability to selectively populate anatomically appropriate regions of the lung, we assessed the location and density of cells over time. Rat lungs were decellularized to remove cellular components and visible nuclei (Fig. 2A, B). After initial seeding and 1 day of culture, cells are noted throughout the alveoli, both as single cells and clusters (Fig. 2C, inset). These cells do not inhabit the small airways (Fig. 2D, arrow), nor do they enter the vascular compartment. Hence, this observation confirmed prior speculation from our group, and others that epithelial cells reintroduced into an acellular tend to home to correct anatomic locations within the scaffold. Cells exhibit a rounded or cuboidal morphology (Fig. 2C, inset). After 7

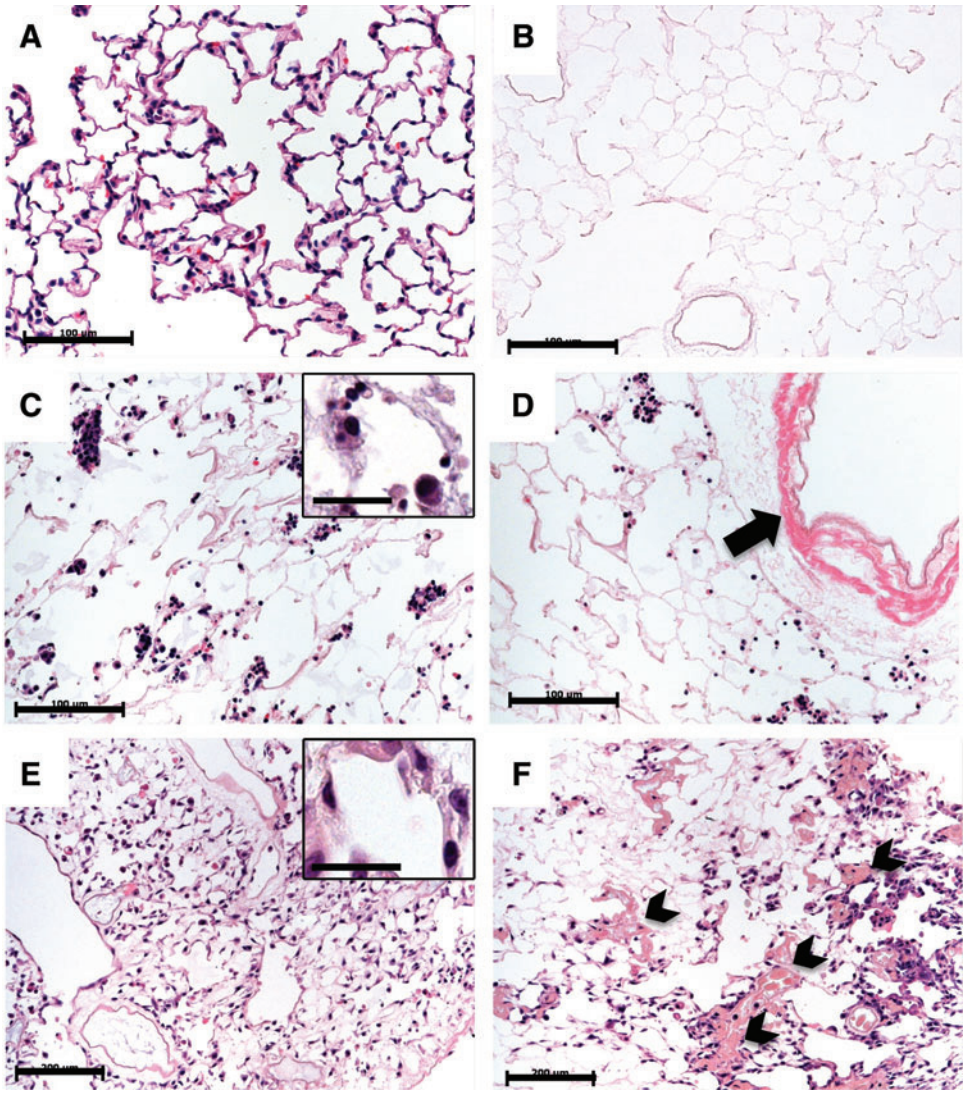

FIG. 2. Hematoxylin and eosin (H&E) stains of native, decellularized, and repopulated lung. **(A)** Native lung. **(B)** Decellularized lung. **(C)** Alveolar areas of a lung scaffold seeded with RTII-70+ cells and cultured for 1 day in Dulbecco's modified Eagle's medium (DMEM) + 10% fetal bovine serum (FBS) with pulsatile perfusion at 1 mL/min. 1E7 cells were seeded in the upper right lobe of the decellularized lung; *inset* shows high magnification of cells adhering to the basement membrane of an alveolus. **(D)** Small airway (*arrow*) of the lung scaffold depicted in **(B)** shows no cellular repopulation of this structure. **(E)** An acellular scaffold after seeding with RTII-70+ cells and cultured for 7 days; *inset* shows high magnification for distinction of cell morphology after 7 days of culture. **(F)** RTII-70+ cells after 7 days of culture on decellularized lung. Eosinophilic foci are indicated (*chevrons*). Scale bars = 100 μm. Scale bars, *insets* = 25 μm. Color images available online at www.liebertpub.com/tea

days in culture, the cells cover the ECM more densely and with a more even distribution (Fig. 2E). Some cells appear to adopt a more elongated phenotype (Fig. 2E, inset). Dense areas of eosinophilic matrix are also present at day 7 (Fig. 2F, chevrons).

Immunostaining of the native and repopulated lung revealed that the cultures stain positively for RTII-70 at day 1 in approximately anatomically correct locations (Fig. 3A, D, inset of D), but this expression is lost after 7 days in culture (Fig. 3G, inset). Pro-SPC appears abundant and appropriately organized, as characterized by punctate surfactant staining throughout the cytoplasm at day 1 (Fig. 3B, E, inset of E). After 7 days in culture, however, the appearance of positive pro-surfactant protein becomes more diffusely distributed throughout the cytoplasm and is diminished in intensity, likely reflecting a nonfunctional phenotype (Fig. 3H, inset). Indeed, diffuse cytoplasmic staining of SPC is associated with surfactant dysfunction disorders, often as a result of trafficking abnormalities.[16] Expression of AQP-5 is scant at day 1 compared with native lung (Fig. 3C, F, inset) and is completely absent at day 7 by immunofluorescence (Fig. 3I, inset). These data suggest that the epithelial cells that initially displayed markers of type II alveolar epithelial cells are not only no longer functional type II cells but that they are also not losing this phenotype in favor of expected progeny such as type I epithelial cells.

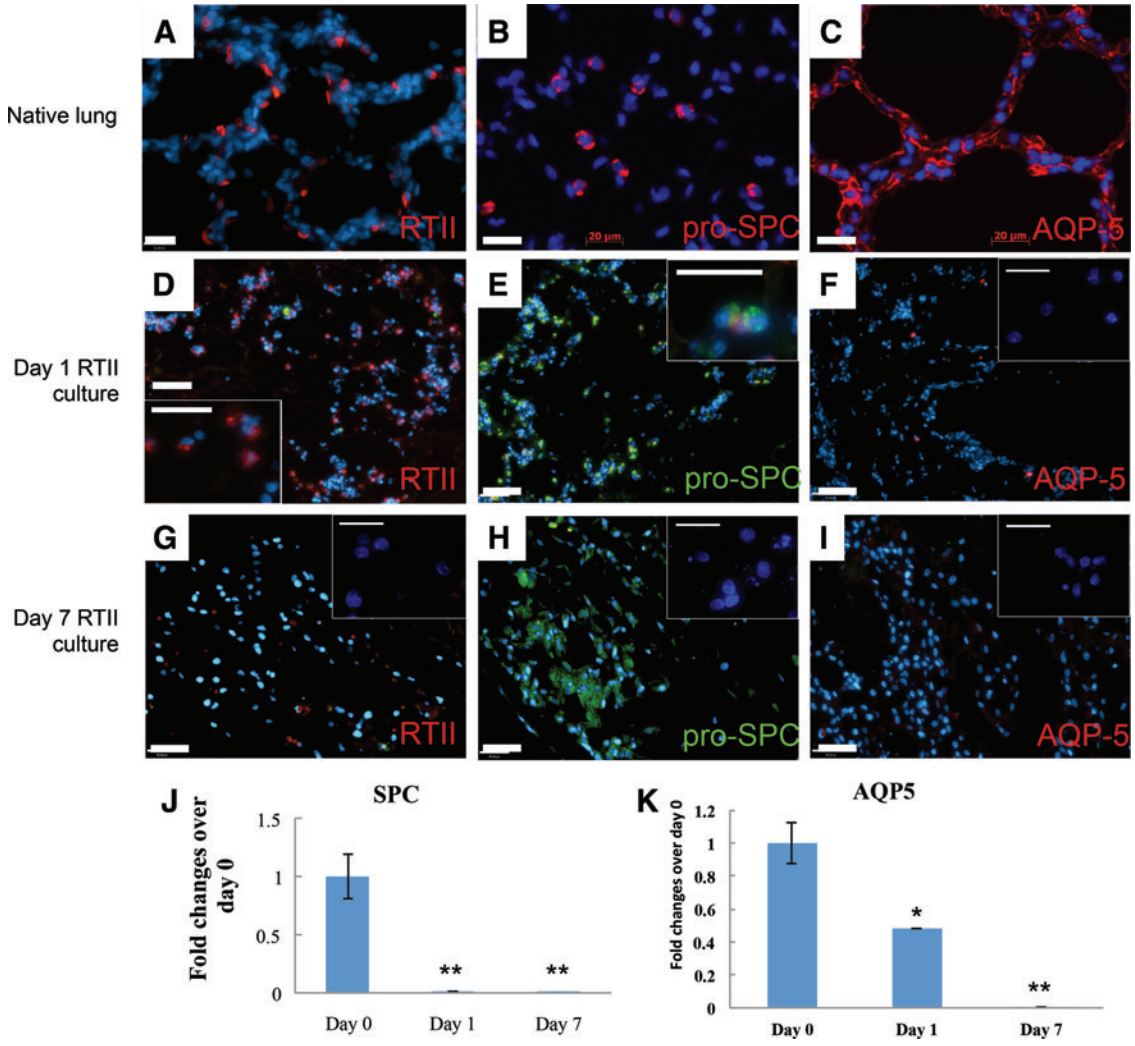

FIG. 3. Expression of alveolar epithelial markers. **(A–C)** Native lung stained for RTII-70 (RTII-70, A), pro-SPC **(B)**, or AQP-5 **(C)**. **(D–F)** Day 1 culture of RTII-70 isolate on decellularized lung stained for RTII-70 **(D)**, pro-SPC **(E)**, or AQP-5. **(G–I)** RTII-70 culture after 7 days stained for RTII-70 **(G)**, pro-SPC **(H)**, or AQP-5 **(I)**. *Insets* are provided in **(D–I)** for visualization of cell morphology at high magnification. Antigen of interest is shown in *red* or *green* [one color per *panel* or *inset*, with the exception of *inset* in **(E)**; color of interest in *inset* **E** is *green*]. Nuclei are stained with 4′,6-diamidino-2-phenylindole (DAPI; *blue*). Scale bars = 20 µm **(A–C)**; 50 µm **(D–I)**. Scale bars, *insets* = 25 µm. **(J, K)** Gene expression by quantitative real-time reverse transcription polymerase chain reaction (qRT-PCR) for *SPC* **(J)** or *AQP5* **(K)**. Gene expression was normalized to *GAPDH* and is expressed as a ratio between the samples of interest and day 0 levels. Fold change is on the y-axis. Sample is indicated below the x-axis. $n = 3$ independent samples. Values are normalized and compared with day 0 (freshly isolated) cells. $p < 0.05$ is indicated by a *single asterisk*; $p < 0.01$ is indicated by *two asterisks*, as determined by Student's *t*-test. Color images available online at www.liebertpub.com/tea

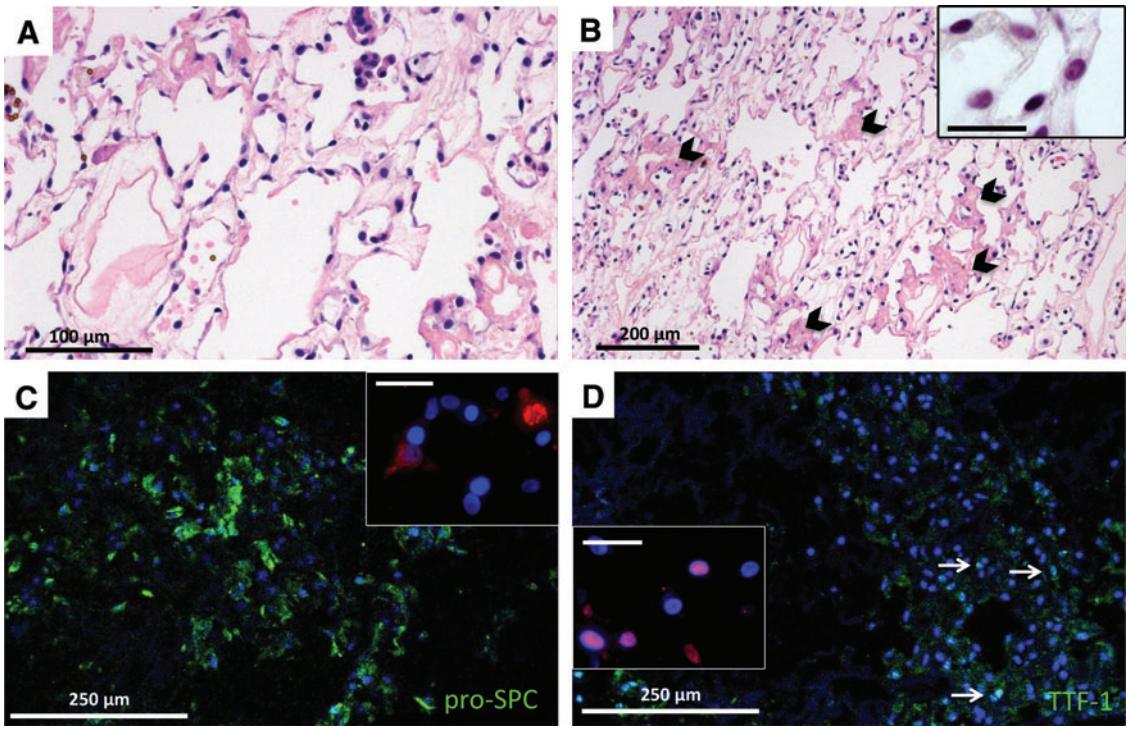

FIG. 4. H&E and immunofluorescent staining for epithelial markers in human type II cells cultured on acellular rat lung matrix. **(A)** H&E of human type II cells cultured on a decellularized rat lung scaffold mounted in a bioreactor and cultured in DMEM + 10% FBS with pulsatile perfusion at 1 mL/min for 7 days. **(B)** Low-magnification H&E of human type II cells cultured on an acellular scaffold for 7 days to show overall distribution. Dense areas of eosinophilic material are indicated (*chevrons*). *Inset* is provided for high magnification. **(C)** Human type II 7-day culture stained for pro-SPC (*green* in *main panel*; *red* in *inset*). **(D)** Human type II 7-day culture stained for thyroid transcription factor-1 (TTF-1; *green* in *main panel*, *red* in *inset*). Nuclei are stained with DAPI **(C, D)**. *Arrows* indicate nuclear localization of TTF-1. Scale bars = 100 μm **(A)**, 200 μm **(B)**, 250 μm **(C, D)**. Scale bars, *insets* = 25 μm. Color images available online at www.liebertpub.com/tea

qRT-PCR analysis for *SPC* demonstrates an ~100× decrease in *SPC* expression after 1 day in culture and nearly 6000× fold decrease by day 7 (Fig. 3J). For *AQP-5*, expression declines 2 and 250-fold at days 1 and 7, respectively, compared with the initial isolated population (Fig. 3K). This suggests a loss of any type I cells initially present and also implies an overall deficiency in type II cells differentiating to type I cells. In sum, these data indicate a loss of definitive epithelial cell markers after culture on the acellular scaffold under these culture conditions (DMEM + 10% FBS, with perfusion of the scaffold with culture medium, but with no ventilation).

Human type II cells cultured on decellularized scaffolds mimic the loss of epithelial markers exhibited by rat distal epithelial cells

Interestingly, human type II epithelial cells that are cultured on decellularized rat matrices displayed a trend in appearance and protein expression that is similar to the rat epithelial cell cultures. As observed in rat RTII-70 cultures, on H&E staining, the human cells were spread over a large portion of the total scaffold (Fig. 4A, B). The presence of elongated cells was noted as they were in the rat cell cultures, but there were also still many cells that displayed a more rounded or cuboidal morphology reminiscent of an epithelial phenotype (Fig. 4A, B, inset of B). Like the rat RTII-70 cultures, there were also areas of dense eosinophilic matrix present after 7 days of culture (Fig. 4B, chevrons). Immunostaining in 7-day cultures was performed for pro-SPC, for thyroid transcription factor-1 (TTF-1), and T1α, a marker of type I epithelial cells. At the 7-day time point, pro-SPC was located somewhat diffusely throughout the cytoplasm of the cells in the scaffold, but had not lost as much intensity in the staining as the rat cells did (Fig. 4C, inset). TTF-1 was found localized to the nucleus in a few rare cells in 7-day cultures (Fig. 4D, arrows and inset), but not in the majority of the population. Additional nonspecific or diffuse cytoplasmic staining is also seen. There was no evidence of T1α staining (data not shown).

Rat epithelial cells gain expression of mesenchymal markers

We assayed cultures of rat epithelial cells over time for the mesenchymal markers, α-actin, vimentin, and TGF-β receptor I. The type I TGF-β receptor is not constitutively active, but forms a heterodimer with the constitutively active type II receptor when it binds to TGF-β. An active TGF-β I receptor is required for phosphorylation and activation of Smad proteins, which are thought to be key mediators of epithelial–mesenchymal transition (EMT). In contrast to the diminished expression of epithelial markers in our system, mesenchymal markers show increased expression in samples of rat cells cultured on the decellularized matrix at both the protein and RNA levels. Staining of

rat cell cultures for α-actin, largely absent at day 1, increases dramatically by day 7 (Fig. 5C, E, with corresponding high-magnification inset panels; Fig. 5A shows native rat lung stained for α-actin). After 7 days in culture, nearly all of the rat cells within the lung are α-actin positive. Gene expression in these samples indicates an increase in *α-actin* of approximately five-fold ($p = 0.00049$) after 1 day in culture and eight-fold by day 7 ($p = 1.4E\text{-}10$; Fig. 5G).

Vimentin expression is already apparent and quite abundant after 1 day in culture, at both the protein (Fig. 5D, inset, similar to native lung Fig. 5B) and gene levels for these cells (Fig. 5H). Gene expression of this cytoskeletal component increases by 2.6-fold ($p = 0.00055$) after 1 day in culture. By day 7, *vimentin* transcript expression decreases relative to day 1 and is not significantly different from expression levels found in freshly isolated cells ($p = 0.16$). However, vimentin protein persists at levels detectable by immunofluorescence (Fig. 5F, inset). Transcript levels for *TGF-βR* increase after 1 day in culture compared with freshly isolated cells ($p = 2.3E\text{-}5$) and remain significantly elevated at day 7 ($p = 0.00021$; Fig. 5I). Taken together, these data suggest that the cells seeded into the scaffold at day 0 undergo EMT that begins as early as 1 day in culture.

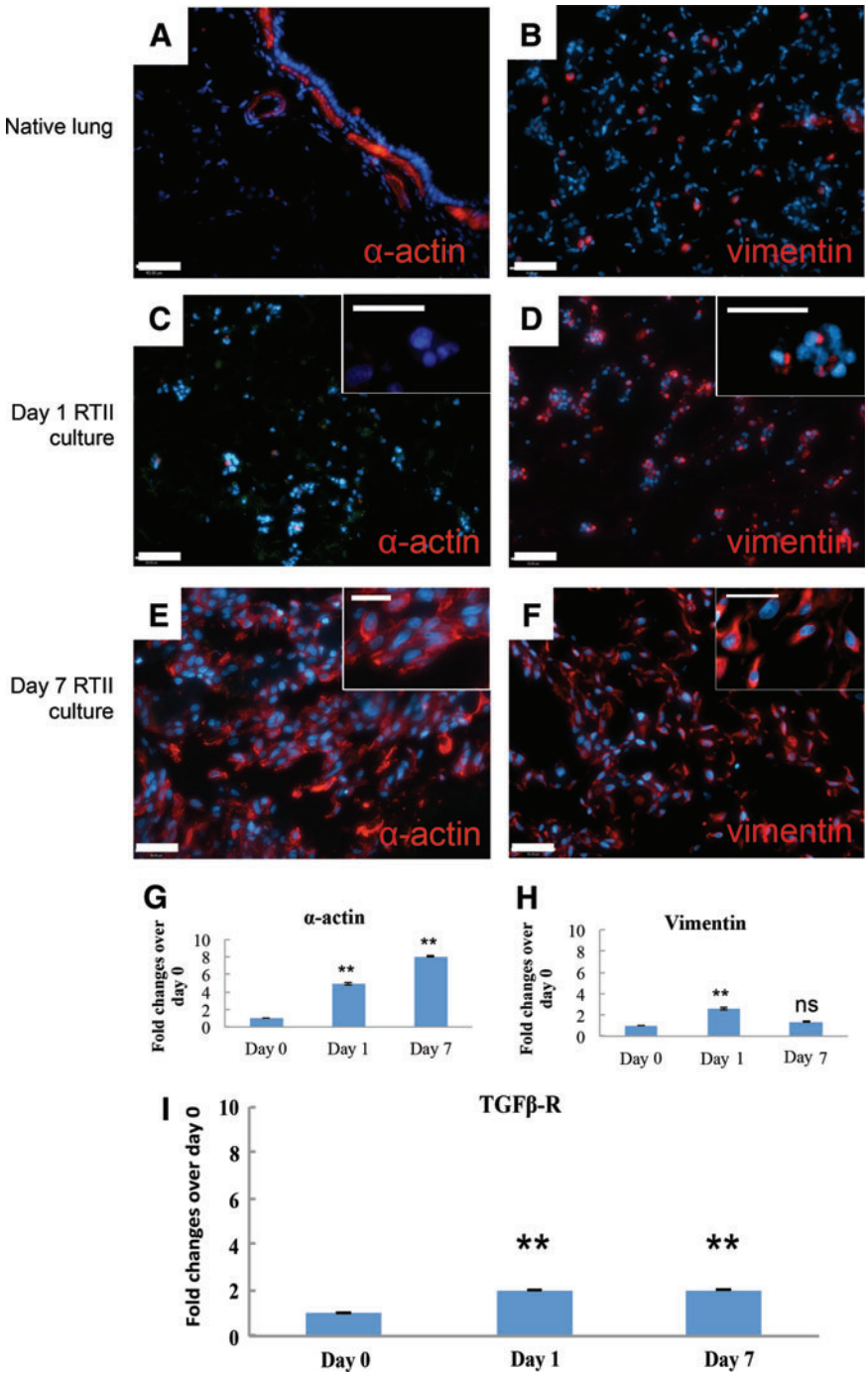

FIG. 5. Expression of mesenchymal markers. (A, B) Native lung stained for α-actin **(A)** or vimentin **(B)**. **(C, D)** One-day cultures of RTII-70 isolate on decellularized lung stained for α-actin **(C)** or vimentin **(D)**. **(E, F)** Seven-day cultures of RTII-70 isolate on decellularized lung stained for α-actin **(E)** or vimentin **(F)**. *Insets* are included in **(C–F)** to provide visualization of cell morphology at high magnification. Antigens of interest are in *red*. Nuclei are counterstained with DAPI (*blue*). Scale bars = 50 μm **(A–F)**. **(G–I)** qRT-PCR gene expression for *α-actin*, *vimentin*, and *TGF-β receptor*. Gene expression was normalized to *GAPDH* and is expressed as a ratio between the samples of interest and day 0 levels. Fold change is on the y-axis. Sample is indicated below the x-axis. $n = 3$ independent samples. Values are normalized and compared with day 0 (freshly isolated) cells. $p < 0.01$ is indicated by *two asterisks*, as determined by Student's *t*-test. ns, no significant difference. Scale bars, *insets* = 25 μm. Color images available online at www.liebertpub.com/tea

Human epithelial cells express the mesenchymal marker, vimentin, and the signal transduction molecule, pSmad2

In contrast to the expression of α-actin by rat epithelial cells in culture, human type II cells cultured on the decellularized rat matrix were negative for the mesenchymal protein, α-actin, after 7 days in culture (Fig. 6A). However, there was some expression of vimentin, another cytoskeletal protein associated with mesenchymal cells after 7 days in culture (~40–50% of all cells; Fig. 6B). Approximately half of the human cells cultured in the decellularized matrix were PCNA positive, indicating that there is a proliferative fraction in the population (Fig. 6C). Finally, human type II cells cultured in the decellularized matrix show nuclear localization of the phosphorylated signal transduction molecule, Smad2 (pSmad2; Fig. 6D–F). Nuclear localization of the phosphorylated form of this molecule is a direct result of active TGF-β signaling. Therefore, these data suggest that the human epithelial cells in these cultures are binding TGF-β in culture likely from serum, thereby activating the ALK5 signaling pathway.

Rat cells and the ECM

A switch to a mesenchymal phenotype can also be driven by ECM components. To further characterize and evaluate the interaction of the cells with the ECM, we evaluated the distribution and abundance of the key ECM proteins and matrix metalloproteases by immunostaining for fibronectin, collagen IV, and MMP-2. *Fibronectin* and *MMP-2* were also evaluated by gene expression. *Collagen I* abundance was assessed at the transcript level only.

Fibronectin is a key component of the provisional matrix that epithelial cells adhere to and migrate over during wound healing.[17,18] It also accumulates at the site of injury during a fibrotic response.[19] After 1 day in culture in our system, there is little fibronectin apparent (Fig. 7D). At this short time point, any fibronectin that is there is likely from the serum-containing culture medium since serum has high levels of soluble fibronectin.[2] However, gene expression for fibronectin does increase by day 1 ($p=0.0135$; Fig. 7K), and by day 7, there appears to be an increase in protein expression as well, especially in areas highly populated by the rat cells cultivated within the matrix (Fig. 7G).

Collagen IV is a key basement membrane protein (Fig. 7B, E, H),[20,21] and MMP-2, also known as gelatinase A or type IV collagenase, breaks down this matrix component. Epithelial cells do not constitutively express this enzyme. Accordingly, neither native lung samples (Fig. 7C) nor day 1 cultures (Fig. 7F) contain positive MMP-2 staining. By day 7, however, there is decreased immunostaining for collagen IV and positive staining for MMP-2 (Fig. 7H, I). Therefore, this enzyme activity is acquired over time in culture. Gene expression for *MMP-2* indicates a significant increase at day 1 ($p=0.0128$), followed by a decline to initial cell isolate levels by day 7 ($p=0.3840$; Fig. 7L). By day 7, immunostaining for collagen IV has a degraded appearance indicative of ongoing matrix breakdown, while MMP2 is widely expressed by immunostaining. In contrast, expression of the *collagen I* gene increases over time and remains significantly elevated at day 7 compared with cell isolates ($p=0.0016$; Fig. 7J), implying ongoing deposition of this matrix protein that is typically deposited by mesenchymal cells.

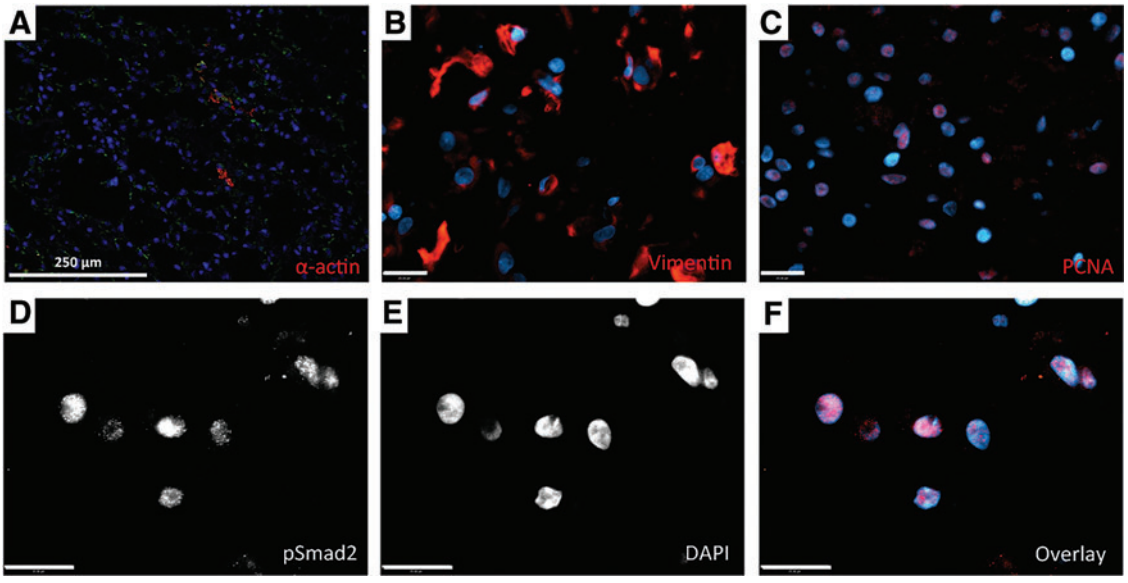

FIG. 6. Mesenchymal markers and nuclear markers in human type II cell cultures. **(A)** Human type II culture stained for α-actin (*red*) after 7 days of bioreactor culture with pulsatile perfusion at 1 mL/min. **(B)** Human type II culture stained for vimentin (*red*). **(C)** Human type II culture stained for proliferating cell nuclear antigen (PCNA; *red*). **(D)** Human type II culture stained for phosphorylated Smad2 (pSmad2); *red* channel is displayed. **(E)** DAPI nuclear counterstain for pSmad2 staining. **(F)** Overlay of pSmad2 and DAPI for human type II culture at 7 days. Nuclei are stained with DAPI **(A–C, E, F)**. Scale bars = 250 μm **(A)**, 25 μm **(B–F)**. Color images available online at www.liebertpub.com/tea

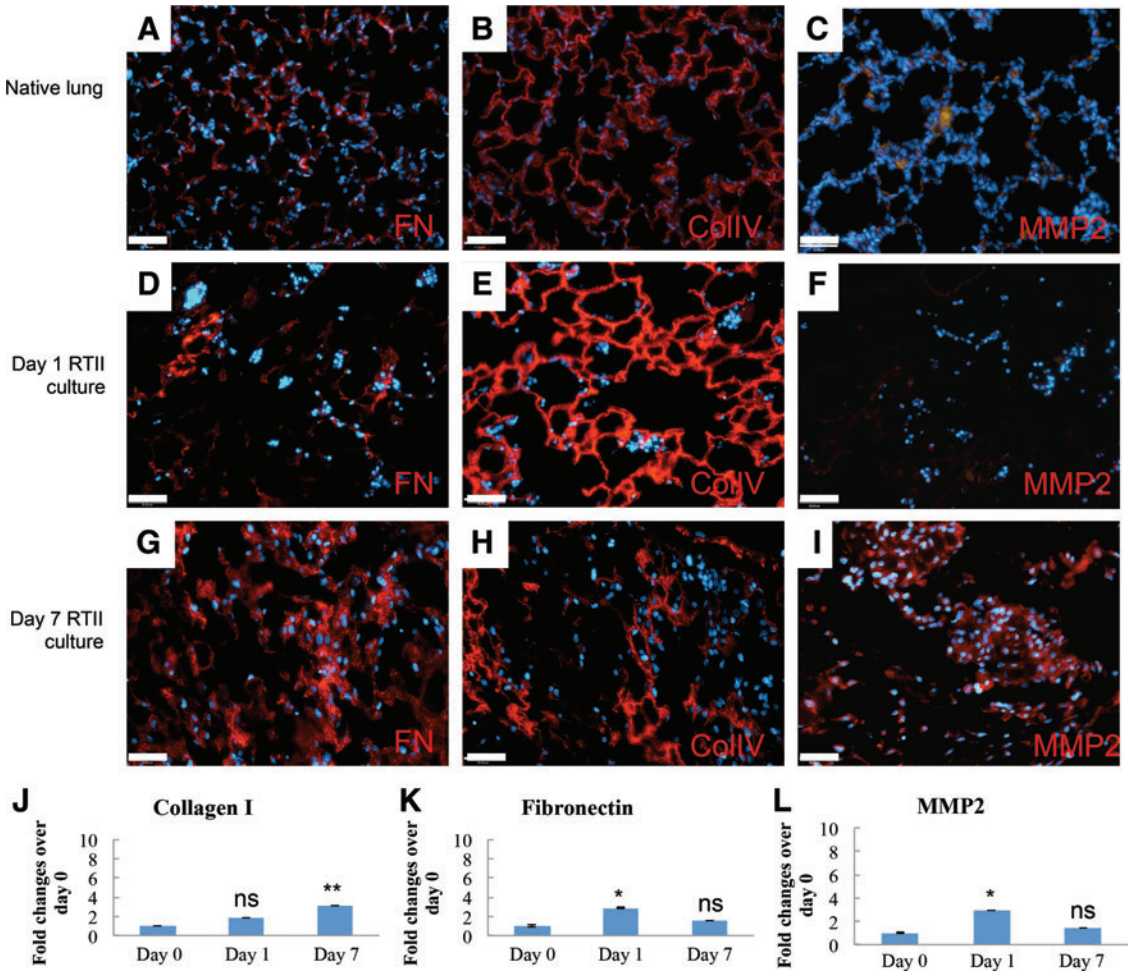

FIG. 7. Extracellular matrix staining and gene expression for native lung and RTII-70 cultures after 1 and 7 days. **(A)** Immunofluorescence of native lung stained for fibronectin (*red*). **(B)** Native lung stained for collagen IV (*red*). **(C)** Native lung stained for matrix metalloprotease-2 (MMP-2). **(D–F)** One-day culture of RTII-70 isolate on decellularized lung stained for fibronectin **(D)**, collagen IV **(E)**, or MMP-2 **(F)**. **(G–I)** Seven-day culture of RTII-70 isolate on decellularized lung stained for fibronectin **(G)**, collagen IV **(H)**, or MMP-2 **(I)**. All antigens of interest are shown in *red*. Nuclei are stained with DAPI (*blue*). Scale bars = 50 μm **(A–I)**. **(J–L)** Gene expression by qRT-PCR for *collagen I* **(J)**, *fibronectin* **(K)**, and *MMP-2* **(L)**. Gene expression was normalized to *GAPDH* and is expressed as a ratio between the samples of interest and day 0 levels. Fold change is on the y-axis. Sample is indicated below the x-axis. All values are normalized to day 0 (freshly isolated) cells. $n = 3$ independent samples. Values are normalized and compared with day 0 (freshly isolated) cells. $p < 0.05$ is indicated by a *single asterisk*; $p < 0.01$ is indicated by *two asterisks*, as determined by Student's *t*-test. Color images available online at www.liebertpub.com/tea

Discussion

Type I and type II alveolar epithelial cells are critical to the generation of functional lung tissue. In our prior studies, seeding of acellular rat lung scaffolds with mixed populations of neonatal rat lung cells (containing SPC-, CCSP- CD31-, and alpha-actin-positive cells) resulted in region-specific matrix repopulation and overall retention of epithelial cell phenotypes and markers. Studies with isolated rat type II cells on decellularized human matrix by Lwebuga-Mukasa *et al.* demonstrated a shift from a type II phenotype to a cell type with a more flattened morphology than that of a typical cuboidal type II cell; the cells cultured by this group also demonstrated reduced phospholipid production.[8] Lacking additional information, the authors concluded that this change in cell type might be a recapitulation of the differentiation of type II cells to type I cells that has been observed *in vivo* after injury.

In this study, seeding a population of distal lung cells that are enriched for type II alveolar epithelial marker, RTII-70, into a decellularized scaffold and culturing the construct for up to 7 days resulted in a similar flattening change in morphology as well as diminished pro-SPC production. However, evaluation of the cells by protein and RNA indicates that the cells lose expression of alveolar epithelial markers and gain near-universal expression of mesenchymal markers after 7 days. These changes were noted qualitatively by immunostaining and quantitatively using qRT-PCR. Based upon these observations and the very scant proportion of alpha-actin-positive cells in the initial cell population, we hypothesize that these cells undergo an epithelial-to-mesenchymal transition when seeded into the lung matrix as a

purified cell source. Although similar in appearance to the flattened morphology of a type I-like cell, the resulting mesenchymal phenotype is different from that of an epithelial or epithelial-like cell. This has functional consequences both for repopulating the alveolar compartment with the aim of creating functional lung tissue that can exchange gas and for the impact that these cells have on the architecture of the scaffold in which they reside.

Of the mesenchymal markers investigated here, vimentin is the first to be detected at the protein level. After 1 day in culture, a large portion of the total cells that are distributed within the scaffold are vimentin positive. Although other mesenchymal markers are not widely expressed at the protein level until day 7, this time frame for vimentin is consistent with *in vitro* studies of induced EMT. In prior studies, alveolar type II cells isolated from adult Sprague-Dawley rats express vimentin protein within 4 h of treatment with TGF-β, and by 24 h, most cells possessed intact vimentin filament networks.[22] In response to soluble collagen IV, another EMT stimulus, human mammary epithelial cells and breast cancer cells have increased vimentin protein expression by 3 h.[23] Therefore, these data suggest that the epithelial cells that are seeded onto the decellularized matrix may have already initiated an EMT program after 1 day and that the vimentin present at the gene and protein levels is the harbinger of this process.

Overall, the loss of an epithelial phenotype of cells cultured on the acellular matrix was somewhat unexpected. Compared with culture of primary epithelial cells on tissue culture plastic, the decellularized lung matrix is softer and contains more tissue-specific proteins. Both of these factors have been shown to promote the tissue-specific cell phenotype and function.[24–28] Clearly, in the experiments presented here, the ECM is not sufficient under the culture conditions used (DMEM + 10% FBS, perfusion, no ventilation) to maintain neonatal, rat lung epithelial phenotypes. Instead, these cells appear to undergo an EMT. Two key differences between prior studies and the studies presented here include the use of ventilation and of a more highly mixed cell population.

Lack of ventilation in these studies compared with whole lung experiments reported previously[2] may be significant as the benefits of stretch on epithelial phenotypes are well documented. Early lung development is characterized by fetal breathing movements (FBM) that keep the lung expanded to a volume up to twice that of postnatal functional residual capacity,[29] and lack of FBM leads to lung hypoplasia during development.[30] Additionally, distension favors expression of the type I alveolar epithelial cell phenotype, the cells most important for gas exchange in the lung,[31] while variable stretch can increase surfactant secretion by type II alveolar epithelial cells.[32] In our system, ventilation with culture medium may also confer benefits with respect to nutrient and oxygen transport. This may have played a role in the observed EMT as physiological stress and hypoxia may be involved in inducing EMT.

In addition to the role played in cellular phenotypic maintenance by ventilation, the medium and the components included or absent in it may also play a role in the observed phenotypic shift. The presence of TGF-β in serum is known to be present at concentrations of up to 2 ng/mL of TGF-β in DMEM containing 10% FBS.[33] This is the same concentration of TGF-β used by Rogel *et al.* to induce EMT in rat type II cells isolated from adult Sprague-Dawley rats.[22] Previous studies have shown that the addition of TGF-β to isolated rat type II cells cultured *in vitro*, or to bronchial epithelial cells, leads to EMT. Conversion of the type II cells to a mesenchymal phenotype occurred within 6 days.[34] Bronchial cells maintained an epithelial phenotype after 1 day in culture with TGF-β, but adopted a spindle-shaped morphology and showed increased expression of mesenchymal markers at 7 days.[35] In a mouse model of pulmonary fibrosis that relies on overexpression of active TGF-β, clusters of X-gal (to identify cells of epithelial origin) and α-smooth muscle actin-positive cells are frequently located in areas of dense fibronectin deposition, and when isolated murine type II epithelial cells were cultured *in vitro* on fibronectin, they underwent EMT through $\alpha_v\beta_6$ integrin activation of secreted latent TGF-β.[36]

In contrast, the presence of all-trans retinoic acid, a common component of media used to support epithelial phenotypes, can limit the levels of phosphorylated Smad 2 and 3 that are induced by active TGF-β1 in differentiating hematopoietic cells.[37] BMP-7 is also a candidate for prevention of EMT through TGF-β inhibition. Studies show that BMP-7 can inhibit TGF-β-induced EMT in renal fibrosis,[38] although reports of efficacy in models of pulmonary fibrosis are mixed.[39,40] Mitigating these observations regarding TGF-β, however, is the fact that our prior studies of cell culture on rat lung scaffolds also utilized DMEM with 10% serum, and in the case of mixed epithelial cultures, we did not observe EMT as described here. Hence, if TGF-β is causative, it is likely in concert with another cue such as lack of (some unknown) supporting cell types that were present in mixed cultures, yet lacking in purified RTII-70+ populations.

Finally, ECM components are nontrivial constituents of the microenvironment. Both native collagen IV and fibronectin can induce EMT in epithelial cells. Treatment of epithelial cells with soluble native collagen IV induces NF-κB activation and an increase in MMP-2 secretion.[23] Fibronectin, although minimally present in the scaffold used here,[2] is present in soluble form in FBS. Fibronectin can induce EMT through activation of the $\alpha_6\beta_4$ integrin, which activates latent TGF-β that then acts on the overlying epithelial cells.[36] In the absence of other potent stimuli such as ventilation or paracrine factors, the soluble fibronectin, or the possibly fragmented collagen IV in the acellular matrix, may become a dominant factor in driving a mesenchymal phenotype.

The human type II cells cultured on the decellularized lung matrix have a similar appearance to the rat RTII-70+ isolate cultured on the decellularized matrix. Based on the immunostaining, however, it appears that these cells do not completely transition from an epithelial to a mesenchymal phenotype over the 7 days of these experiments. This may be due to the difference in age of the cells. Human type II cells were obtained from 50 to 60 year olds, while the rat type II cells are from neonates and hence may have more plasticity. Indeed, alveolar development in rats occurs primarily postnatally, and so is underway at the time the RTII-70+ cells are isolated. Alternatively, differences in the isolation procedures used to obtain rat and human cells may explain the differential expression of epithelial and mesenchymal markers.

With respect to composition of the population, there are some caveats of the rat epithelium-enriched population

described in these studies. First, although type II pneumocytes make up the majority of the population, as indicated by the RTII-70+ population, they are not the sole cell type in these isolates. This leaves the possibility that instead of cells that undergo a shift from an epithelial to a mesenchymal phenotype, the observed increase in mesenchymal gene and protein expression may reflect overgrowth of existing α-actin-positive cells, although not all cells are PCNA positive (data not shown). With regard to type II alveolar epithelial cells, even if the population was 100% RTII-70+ cells, recent evidence has demonstrated the heterogeneity of type II cells,[41] which may mean that some cells have a greater capacity for regeneration than others. Parsing out type II subpopulations and their potential role in EMT and matrix production, as opposed to tissue regeneration, may be an interesting source of inquiry in the future. The use of lineage-traced SPC-cre/reporter mouse cells to definitively show that the originating cell that gives rise to the mesenchymal cells observed at day 7 is, indeed, of type II epithelial origin would also be of interest.

In summary, we have demonstrated the isolation of a population of neonatal rat lung cells enriched for type II epithelial cells or their progenitors by the use of the RTII-70 surface antibody. We seeded these cells into a decellularized lung scaffold and cultured them for 1 or 7 days. During this time, the cells appear to have undergone EMT, which may be part of a wound-healing or Type 2 EMT response. In the quest to reconstitute functional lung tissue, this work represents a new element of cell–cell and cell–matrix interactions that should inform future studies of epithelial and perhaps endothelial cells aimed at repopulating whole lung scaffolds. Further investigation should focus on both shorter and longer time points than those reported here (hours, days 14 and 21). In addition, the impact of media components and physical stimuli such as ventilation are important avenues for additional study. Understanding each of these components in greater depth should improve our ability to refine our cell source selection as well as aid in the selection and delivery of cues required for appropriate cell and tissue organization and function.

Acknowledgments

The authors gratefully acknowledge the gift of RTII-70 antibody from Leland Dobbs and appreciate the time and assistance of Robert Gonzalez in troubleshooting the isolation protocol established for the selection of RTII-70+ epithelial cells. This work was supported by U01 HL111016 and by R01 HL098220 (both to L.E.N.) and by CT Stem Cell # 13SCA36 (to SS).

Disclosure Statement

L.E.N. has a financial interest in Humacyte, Inc., a regenerative medicine company. Humacyte did not fund these studies, and Humacyte did not affect the design, interpretation, or reporting of any of the experiments herein.

References

1. Ott, H.C., Clippinger, B., Conrad, C., Schuetz, C., Pomerantseva, I., Ikonomou, L., Kotton, D., and Vacanti, J.P. Regeneration and orthotopic transplantation of a bioartificial lung. Nat Med **16,** 927, 2010.
2. Petersen, T.H., Calle, E.A., Zhao, L., Lee, E.J., Gui, L., Raredon, M.B., Gavrilov, K., Yi, T., Zhuang, Z.W., Breuer, C., Herzog, E., and Niklason, L.E. Tissue-engineered lungs for in vivo implantation. Science **329,** 538, 2010.
3. Jensen, T., Roszell, B., Zang, F., Girard, E., Matson, A., Thrall, R., Jaworski, D.M., Hatton, C., Weiss, D.J., and Finck, C. A rapid lung de-cellularization protocol supports embryonic stem cell differentiation *in vitro* and following implantation. Tissue Eng Part C Methods **18,** 632, 2012.
4. Price, A.P., England, K.A., Matson, A.M., Blazar, B.R., and Panoskaltsis-Mortari, A. Development of a decellularized lung bioreactor system for bioengineering the lung: the matrix reloaded. Tissue Eng **16,** 2581, 2010.
5. Cortiella, J., Niles, J., Cantu, A., Brettler, A., Pham, A., Vargas, G., Winston, S., Wang, J., Walls, S., and Nichols, J.E. Influence of acellular natural lung matrix on murine embryonic stem cell differentiation and tissue formation. Tissue Eng **16,** 2565, 2010.
6. Daly, A.B., Wallis, J.M., Borg, Z.D., Bonvillain, R.W., Deng, B., Ballif, B.A., Jaworski, D.M., Allen, G.B., and Weiss, D.J. Initial binding and recellularization of decellularized mouse lung scaffolds with bone marrow-derived mesenchymal stromal cells. Tissue Eng Part A **18,** 1, 2012.
7. Longmire, T.A., Ikonomou, L., Hawkins, F., Christodoulou, C., Cao, Y., Jean, J.C., Kwok, L.W., Mou, H., Rajagopal, J., Shen, S.S., Dowton, A.A., Serra, M., Weiss, D.J., Green, M.D., Snoeck, H.-W., Ramirez, M.I., and Kotton, D.N. Efficient derivation of purified lung and thyroid progenitors from embryonic stem cells. Cell Stem Cell **10,** 398, 2012.
8. Lwebuga-Mukasa, J.S., Ingbar, D.H., and Madri, J.A. Repopulation of a human alveolar matrix by adult rat type II pneumocytes *in vitro*. A novel system for type II pneumocyte culture. Exp Cell Res **162,** 423, 1986.
9. Dobbs, L.G., Pian, M.S., Maglio, M., Dumars, S., and Allen, L. Maintenance of the differentiated type II cell phenotype by culture with an apical air surface. Am J Physiol **273(2 Pt 1),** L347, 1997.
10. Gonzalez, R., Yang, Y.H., Griffin, C., Allen, L., Tigue, Z., and Dobbs, L. Freshly isolated rat alveolar type I cells, type II cells, and cultured type II cells have distinct molecular phenotypes. Am J Physiol Lung Cell Mol Physiol **288,** L179, 2005.
11. Gonzalez, R.F., and Dobbs, L.G. Isolation and culture of alveolar epithelial type I and type II cells from rat lungs. Methods Mol Biol **945,** 145, 2012.
12. Calle, E.A., Petersen, T.H., and Niklason, L.E. Procedure for lung engineering. J Vis Exp e2651, 2011.
13. Rice, W.R., Conkright, J.J., Na, C.-L., Ikegami, M., Shannon, J.M., and Weaver, T.E. Maintenance of the mouse type II cell phenotype *in vitro*. Am J Physiol Lung Cell Mol Physiol **283,** L256, 2002.
14. Bove, P.F., Grubb, B.R., Okada, S.F., Ribeiro, C.M., Rogers, T.D., Randell, S.H., O'Neal, W.K., and Boucher, R.C. Human alveolar type II cells secrete and absorb liquid in response to local nucleotide signaling. J Biol Chem **285,** 34939, 2010.
15. Ito, Y., Correll, K., Schiel, J.A., Finigan, J.H., Prekeris, R., and Mason, R.J. Lung fibroblasts accelerate wound closure in human alveolar epithelial cells through hepatocyte growth factor/c-Met signaling. Am J Physiol Lung Cell Mol Physiol **307,** L94, 2014.

16. Wert, S.E., Whitsett, J.A., and Nogee, L.M. Genetic disorders of surfactant dysfunction. Pediatr Dev Pathol **12,** 253, 2009.
17. Garat, C., Kheradmand, F., Albertine, K.H., Folkesson, H.G., and Matthay, M.A. Soluble and insoluble fibronectin increases alveolar epithelial wound healing *in vitro*. Am J Physiol **271,** L844, 1996.
18. Limper, A.H., and Roman, J. Fibronectin. A versatile matrix protein with roles in thoracic development, repair and infection. Chest **101,** 1663, 1992.
19. Thannickal, V.J., Toews, G.B., White, E.S., Lynch, J.P., 3rd, and Martinez, F.J. Mechanisms of pulmonary fibrosis. Annu Rev Med **55,** 395, 2004.
20. Brown, B., Lindberg, K., Reing, J., Stolz, D.B., and Badylak, S.F. The basement membrane component of biologic scaffolds derived from extracellular matrix. Tissue Eng **12,** 519, 2006.
21. Laurent, G.J. Lung collagen: more than scaffolding. Thorax **41,** 418, 1986.
22. Rogel, M.R., Soni, P.N., Troken, J.R., Sitikov, A., Trejo, H.E., and Ridge, K.M. Vimentin is sufficient and required for wound repair and remodeling in alveolar epithelial cells. FASEB J **25,** 3873, 2011.
23. Espinosa-Neira, R., and Salazar, E.P. Native type IV collagen induces an epithelial to mesenchymal transition-like process in mammary epithelial cells MCF10A. Int J Biochem Cell Biol **44,** 2194, 2012.
24. O'Neill, J.D., Freytes, D.O., Anandappa, A.J., Oliver, J.A., and Vunjak-Novakovic, G.V. The regulation of growth and metabolism of kidney stem cells with regional specificity using extracellular matrix derived from kidney. Biomaterials **34,** 9830, 2013.
25. Birukova, A.A., Tian, X., Cokic, I., Beckham, Y., Gardel, M.L., and Birukov, K.G. Endothelial barrier disruption and recovery is controlled by substrate stiffness. Microvasc Res **87,** 50, 2013.
26. French, K.M., Boopathy, A.V., DeQuach, J.A., Chingozha, L., Lu, H., Christman, K.L., and Davis, M.E. A naturally derived cardiac extracellular matrix enhances cardiac progenitor cell behavior *in vitro*. Acta Biomater **8,** 4357, 2012.
27. DeQuach, J.A., Yuan, S.H., Goldstein, L.S., and Christman, K.L. Decellularized porcine brain matrix for cell culture and tissue engineering scaffolds. Tissue Eng Part A **17,** 2583, 2011.
28. Young, D.A., Choi, Y.S., Engler, A.J., and Christman, K.L. Stimulation of adipogenesis of adult adipose-derived stem cells using substrates that mimic the stiffness of adipose tissue. Biomaterials **34,** 8581, 2013.
29. Harding, R. Fetal pulmonary development: the role of respiratory movements. Equine Vet J Suppl 32, 1997.
30. Inanlou, M.R., Baguma-Nibasheka, M., and Kablar, B. The role of fetal breathing-like movements in lung organogenesis. Histol Histopathol **20,** 1261, 2005.
31. Gutierrez, J.A., Gonzalez, R.F., and Dobbs, L.G. Mechanical distension modulates pulmonary alveolar epithelial phenotypic expression *in vitro*. Am J Physiol **274(2 Pt 1),** L196, 1998.
32. Arold, S.P., Bartolák-Suki, E., and Suki, B. Variable stretch pattern enhances surfactant secretion in alveolar type II cells in culture. Am J Physiol Lung Cell Mol Physiol **296,** L574, 2009.
33. Gong, Z., and Niklason, L.E. Small-diameter human vessel wall engineered from bone marrow-derived mesenchymal stem cells (hMSCs). FASEB J **22,** 1635, 2008.
34. Willis, B.C., Liebler, J.M., and Luby-Phelps, K. Induction of epithelial-mesenchymal transition in alveolar epithelial cells by transforming growth factor-β1: potential role in idiopathic pulmonary fibrosis. Am J Pathol **166,** 1321, 2005.
35. Hosper, N.A., van den Berg, P.P., de Rond, S., Popa, E.R., Wilmer, M.J., Masereeuw, R., and Bank, R.A. Epithelial-to-mesenchymal transition in fibrosis: collagen type I expression is highly upregulated after EMT, but does not contribute to collagen deposition. Exp Cell Res **319,** 3000, 2013.
36. Kim, K.K., Kugler, M.C., Wolters, P.J., Robillard, L., Galvez, M.G., Brumwell, A.N., Sheppard, D., and Chapman, H.A. Alveolar epithelial cell mesenchymal transition develops *in vivo* during pulmonary fibrosis and is regulated by the extracellular matrix. Proc Natl Acad Sci U S A **103,** 13180, 2006.
37. Cao, Z. Levels of phospho-Smad2/3 are sensors of the interplay between effects of TGF-beta and retinoic acid on monocytic and granulocytic differentiation of HL-60 cells. Blood **101,** 498, 2002.
38. Zeisberg, M., Hanai, J.-i., Sugimoto, H., Mammoto, T., Charytan, D., Strutz, F., and Kalluri, R. BMP-7 counteracts TGF-β1–induced epithelial-to-mesenchymal transition and reverses chronic renal injury. Nat Med **9,** 964, 2003.
39. Murray, L.A., Hackett, T.L., Warner, S.M., Shaheen, F., Argentieri, R.L., Dudas, P., Farrell, F.X., and Knight, D.A. BMP-7 does not protect against bleomycin-induced lung or skin fibrosis. PLoS One **3,** e4039, 2008
40. Izumi, N. BMP-7 opposes TGF-1-mediated collagen induction in mouse pulmonary myofibroblasts through Id2. Am J Physiol Lung Cell Mol Physiol **290,** L120, 2005.
41. Lee, J.-H., Kim, J., Gludish, D., Roach, R.R., Saunders, A.H., Barrios, J., Woo, A.J., Chen, H., Conner, D.A., Fujiwara, Y., Stripp, B., and Kim, C.F. SPC H2B-GFP mice reveal heterogeneity of surfactant protein C-expressing lung cells. Am J Respir Cell Mol Biol **48,** 288, 2013.

Address correspondence to:
Laura E. Niklason, MD, PhD
Department of Biomedical Engineering
Yale University
10 Amistad St., Room 301D
New Haven, CT 06520

E-mail: laura.niklason@yale.edu

Received: August 27, 2014
Accepted: March 16, 2015
Online Publication Date: May 4, 2015